

International Conference on Space Optics—ICSO 2018

Chania, Greece

9–12 October 2018

Edited by Zoran Sodnik, Nikos Karafolas, and Bruno Cugny



Semiconductor laser modules for precision spectroscopy applications in space

A. Bawamia

Ch. Kuerbis

R. Smol

A. Wicht



ics0 proceedings



Semiconductor laser modules for precision spectroscopy applications in space

A. Bawamia^{*a}, Ch. Kuerbis^a, R. Smol^a, A. Wicht^{a,b}

^aFerdinand-Braun-Institut, Leibniz-Institut für Höchstfrequenztechnik, Gustav-Kirchhoff-Str. 4, 12489 Berlin, Germany; ^bHumboldt-Universität zu Berlin, Newton-Str. 15, 12489 Berlin, Germany

ABSTRACT

The Ferdinand-Braun-Institute has been developing high-power, narrow-linewidth semiconductor lasers for precision spectroscopy applications in harsh environments for more than ten years. Starting with hybrid-integrated diode laser chips and micro-optics on a ceramic platform for Bose-Einstein condensation experiments in a drop tower, the institute is now developing, qualifying and, in many cases, already delivering fully-packaged, multi-functional modules for application on platforms including sounding rockets, the International Space Station (ISS) and nano-satellites. We present the latest generation of electro-optical modules, which is designed to accommodate any two semiconductor chips. This includes, amongst others, the ECDL-MOPA, where the laser architecture consists of an ECDL and a semiconductor optical amplifier, both hybrid-integrated into a sealed package within a footprint of a conventional smartphone (but with a height of approx. 23 mm). The single-mode, polarization-maintaining optical fiber output delivers, for instance, 570 mW of power and a free-running FWHM linewidth of approximately 30 kHz (within a timescale of 1 ms) at the operating wavelength of 1064.49 nm. One such module has already been successfully launched on a sounding rocket mission in May 2018.

Keywords: Semiconductor lasers, ECDL, packaging, sounding rocket

1. INTRODUCTION

The maturing of quantum optical sensor technology employed in e.g. atom interferometers¹ or atomic clocks² and applied in various field such as time keeping, inertial navigation³, and tests of fundamental physics^{4,5} leads to an increasing interest to put this technology to use in the field. Various national and international initiatives, such as the German QUTEGA, the Dutch QUTech, the UK National Quantum Technologies Program, and the European Quantum Technologies Flagship Initiative, are currently pushing the further advancement of cold-atom-based quantum optical sensor technology for deployment in space from which a surplus of sensitivity can be gained.

Key technology components of each quantum optical sensor are lasers which have to fulfill various requirements of the sensor apparatus with respect to their electro-optical performance, e.g. single wavelength emission at a specific wavelength from the UV to the NIR, spectral stability (linewidth well below the MHz level) and spectral purity (side-mode suppression > 40 dB), as well as optical power (> 1 W, free space to be coupled into (typically) polarization maintaining single-mode optical fibers (PM-SMF)). The experimental environment then imposes further demands on the lasers regarding their mechanical stability (robustness), and the footprint and volume that they take up (compactness). Especially space deployment requires highly reliable and energy-efficient lasers that can be operated after mechanical (rocket launch) and under thermal and radiation stress. Semiconductor lasers provide a promising approach for realization of space-suitable laser systems when combined with micro-integration technologies. GaAs-based diode lasers can cover emission wavelengths ranging from approx. 650 nm up to 1100 nm, while GaN- and InP-based diode lasers allow access to shorter and longer wavelength ranges, respectively. To cover shorter wavelengths, frequency conversion techniques can also be applied. While monolithic diode lasers provide a simple resonator architecture, an improved spectral stability can readily be achieved by choosing an extended or external cavity concept. Employment of diode laser chips and optical amplifier chip in a master-oscillator-power-amplifier (MOPA) setup allows for optical output powers in excess of 1 W⁶. Combination of, e.g., extended cavity diode laser (ECDL) master oscillators with optical amplifiers provides spectrally pure high power laser emission as required by various quantum optical sensors. Hybrid integration of the ECDL-MOPA with beam shaping and distribution micro-optics and fiber-coupling into a sealable housing is a promising approach to realize space-suitable lasers.

This work is supported by the German Space Agency (DLR) with funds provided by the Federal Ministry for Economic Affairs and Energy (BMWi) on the basis of a decision of the German Bundestag (Grants No. 50WM1141, 50WM1434, 50WM1545, 50WM1646, 50WM1755, 50WP1704).

In this contribution, we describe the current status of our efforts to develop a versatile hybrid integration technology platform that could serve as a generic approach to micro-integration of semiconductor-based laser modules for quantum optical sensor applications in space. In section 2, we describe the technology platform for the hybrid micro-integration of any 2 semiconductor chips inside a sealed package. The electro-optical performance of an ECDL-MOPA module emitting at 1064 nm shall be presented in section 3. This ECDL_MOPA laser module was successfully flown on a sounding rocket mission in May 2018 as part of an iodine-based frequency reference deployed in space.

2. TECHNOLOGY PLATFORM FOR MICRO-INTEGRATION OF SEMICONDUCTOR-BASED LASER MODULES

The basic idea behind the technology platform described in this section is to be able to implement almost any electro-optical module that can be realized by means of 2 diode laser chips. This general approach avoids the need to re-design the laser modules when modifications of existing laser concepts or even new concepts have to be implemented, thus reducing cost and development time. Moreover, a new packaging technology has been developed, including electrical and optical feedthroughs, as well as on-board fiber coupling and thermal management. We also developed a micro-mirror concept that is insensitive to adhesive shrinkage and thus enables sub-100nm bonding accuracy.

2.1 Module body conceptual approach

The conceptual approach to the new generation of laser modules rests on versatility and multi-functionality, embodied by a design incorporating two arbitrary semiconductor-based active or passive chips and two optical ports that can be used as input or output ports according to the requirements, see Figure 1. For instance, a MOPA would incorporate a laser chip or even an ECDL, an amplifier chip, and two optical output ports, one behind the rear facet of the laser chip and the other in front of the output facet of the amplifier. The same approach can now be used to build, for example, a double-stage amplifier, consisting of a pre-amplifier and a main amplifier. The optical port behind the entry facet of the pre-amplifier then serves as input port, channeling light from an external laser into the system. After passing through the pre-amplifier and main amplifier, the laser light exits the system through the optical port in front of the main amplifier. Table 1 lists a series of possible combinations of active and passive semiconductor chips that can be implemented in the present laser module concept.

module functionality	Chip 1	Chip 2
DFB-MOPA	DFB	amplifier
DFB laser w/ phase modulator	DFB	phase modulator
ECDL-MOPA	ECDL	amplifier
ECDL w/ phase modulator	ECDL	phase modulator
dual stage optical amplifier	pre-amplifier	main amplifier
phase modulator w/ amplifier	phase modulator	amplifier

Table 1. Selection of possible combinations of active and passive semiconductor chips for implementation into a module.

Figure 1 shows a CAD model of the module body, in this case with chip 1 constituting the gain chip of an ECDL and chip 2 an amplifier. The module body has dimensions of 80×30×10 mm³ and features a mass of about 50 g. A thick AlN ceramic plate serves as a base plate and ensures mechanical stability of the assembly. Above, a thinner, intermediate AlN ceramic plate and finally three narrow AlN ceramic rails together set up the platform used to implement the electro-optical system. The AlN ceramic plates are assembled by flux-free soldering. Patterns of metallization on the AlN ceramic plates are realized with lithographic methods well established for electronic hybrids so that each of the AlN ceramic plates features an electrical functionality similar to what is provided by printed circuits boards. Thanks to the excellent heat conductivity of AlN ceramics even small electric strips feature large ampacity. Integration of through-vias into the AlN plates allows for stacking and hence for implementation of rf-compatible, high ampacity, multi-layer electric layouts. Stacking also provides the means to implement more complex 3D mechanical geometries.

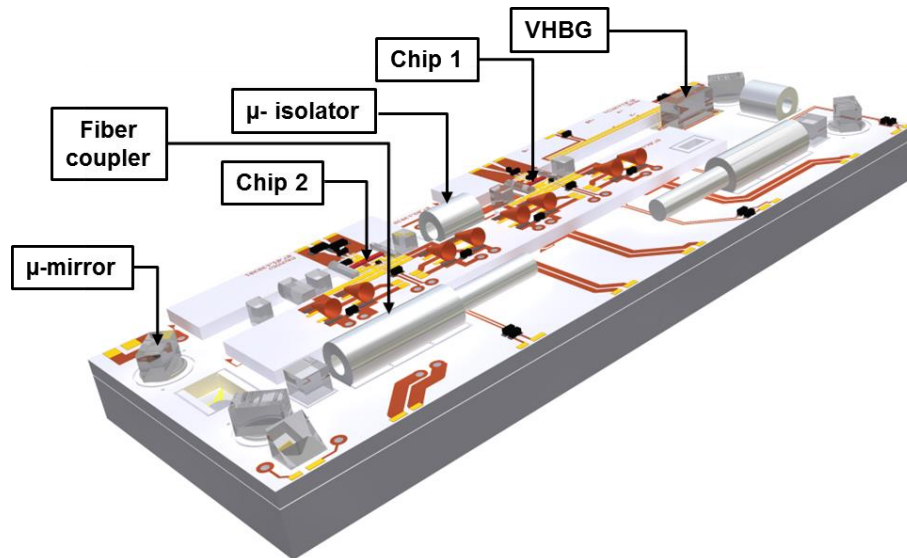


Figure 1. CAD Model of an ECDL-MOPA module with dimensions 30 x 80 x 10 mm³. VHBG: volume holographic Bragg grating; μ -isolator: micro-optical isolator; μ -mirror: micro-mirror. The optical fibers exiting the fiber coupler are not shown in the figure.

The laser diode chips, each of which are either soldered or adhesively bonded on an AlN submount, are integrated inside the space between the rails by adhesive bonding. The intermediate AlN plate and the three rails, together with mechanical structures cut-out inside the AlN, also serve as anchor points for the attachment of the optical components. Electrical connections between chips and the AlN ceramic module body are implemented by conventional Au-wire bonding.

The general principle behind the optical path on the module body is explained via the example of the ECDL-MOPA shown in Figure 1. However, the basic principles behind the beam shaping and beam collection at the optical ports remain the same for all other implementations mentioned in Table 1. For the example discussed here, the local oscillator is implemented by an ECDL, whose resonator is formed by the front facet (facing towards chip 2) of chip 1 and by the effective mirror plane of the volume holographic Bragg grating (VHBG). Intra-cavity lenses collimate the beam exiting the rear facet of chip 1 onto the VHBG, thus creating a stable resonator for the ECDL. Two laser beams exit the ECDL, a main local oscillator beam at the front facet of chip 1 and an auxiliary beam at the rear facet of the VHBG.

The main local oscillator beam is collimated and travels through a μ -isolator before being focused into the waveguide of chip 2, a single-pass power amplifier. The μ -isolator ensures that no stray light, no directly reflected light, and no spontaneous emission of chip 2 is fed back into the local oscillator. At the output of chip 2, the amplified light is collimated before being deflected twice with the help of μ -mirrors positioned at 45° to the beam axis. The beam is subsequently injected into a fiber coupler ferrule, consisting of a coupling lens and a single-mode, polarization-maintaining fiber whose facet lies in the focal plane of the lens. A polarizing beam splitter in front of the fiber coupler filters out the fraction of the optical field oscillating in the undesired polarization. It should be noted that, although a cut-out for a μ -isolator is foreseen between the two μ -mirrors, none is actually implemented. This is because the only μ -isolators existing in the present form factor (\varnothing 4 mm, 5 mm length) have a maximum rating that is well below the intensities provided by the output of chip 2. However, until now, no perturbation of the local oscillator due to feedback into the amplifier has been observed. Depending on the application one has in mind, a fiber-coupled isolator may be added outside the module to provide isolation of the module from optical feedback created by the environment.

The beam exiting the ECDL through the VHBG is, per resonator design, quite collimated. This auxiliary beam path is very similar to that of the main beam emitted by chip 2, except that here a μ -isolator is placed between the two μ -mirrors in order to avoid feedback into the local oscillator through the auxiliary port.

All optical elements are adhesively bonded to the ceramics using UV-cured epoxy adhesives. Since micro-lenses with small focal lengths (from a few 100 μ m to a few mm) are used, the position of the components must be maintained during curing of the adhesive with some 100 nm. This ensures that beam aberrations and clipping are minimized and that optimal collimation or focusing is achieved. When it comes to coupling into the fiber coupler (fiber facet in the focal

plane of the coupling lens), the main constraint is the angle between the beam and the optical axis of the coupler. To first approximation, the angular misalignment between the laser output of chip 2 and the fiber coupler is solely determined by lateral misalignment of the lenses collimating the output of chip 2. In practice, it has been observed that lateral misalignments of lenses in the sub-micrometer range are sufficient to cause a reduction of 10% in the coupling efficiency into the optical fiber.

The bonding technology applied to the micro-lenses on the laser module body does not enable gap-free bonding. As a consequence, misalignment of the optics cannot be avoided during curing, when the adhesive shrinks. At present, the combination of adhesives that are in use and of the geometry and tolerances of the AlN body and of the micro-optical elements the misalignment through shrinkage can be limited to approximately 1 μm . This is definitely not sufficient if optimal fiber coupling efficiency is targeted. Therefore, the micro-mirrors are used to compensate the residual misalignment of the micro-lenses. Although the micro-mirrors are also adhesively bonded, a special, gap-free fixation method developed at the FBH considerably reduces the residual bonding-induced misalignment. We estimate the residual effective misalignment to be well low 100 nm.

The electrical layout of AlN ceramic body allows for operation of chips that feature sections. This provides significant functional versatility: at the position of chip 1, for example, a DBR laser with separate control of the injection current to the Bragg reflector section and to the gain section can be used. Alternatively, a DBR laser chip with integrated heater for the Bragg reflector section could be operated. Also, DBR or Fabry-Perot chips with a long gain section and a short (and fast) modulation or reverse bias voltage section could be integrated (the latter if mode-locking is targeted). At position of chip 2, for example, tapered amplifier chips with separate control of the injection current to the ridge waveguide input mode filter/preamplifier and to the tapered section may be used.

A photodiode is implemented behind the mirror just in front of the main port fiber coupler. This provides to monitor the power injected onto the fiber coupler.

To provide ultra-fast access to the laser diode injection current, wide bandwidth (10 GHz) transistors can either be integrated on the rails or – for the highest frequency requirement – directly on the laser chip submount. In various setup we have demonstrated a 3 dB-bandwidth between 1 and 3 GHz with respect to power modulation. This eases frequency control of the master oscillator and power control at the power amplifier.

To ease thermal control and monitoring of the laser module, a minimum of 3 thermistors is integrated. One is buried with the ceramic body to determine the temperature of the ceramic module body. Each of the chip submounts carries its own thermistor very close to the laser chip so that the chip temperature can be closely monitored.

To provide flexibility for the thermal management a micro-thermo-electric-cooler (TECs) can replace the submount for the laser chip at chip position 1 (TEC.Chip). This allows for temperature control of chip 1 with a time constant of about 0.1 s and thermally decouples chip 1 from the ceramic module body. This is important for implementation of MOPAs based on monolithic master oscillators: here, the chip 1 temperature has to be set to control the emission frequency, while the power amplifier at chip position 2 requires the ceramic module body temperature to be as low as possible to provide the best power efficiency and the highest output power possible. This μTEC also carries a thermistor.

For ECDL applications another micro-TEC can be integrated into the module body to allow for thermal tuning of the VHBG (TEC.VHBG). This TEC carries a thermistor for closed-loop temperature control. The thermistor is buried inside the TEC to reduce thermal cross-talk from the environment.

2.2 Packaging technology

The conceptual approach to the implementation of the housing is based on technology well established for electronic hybrids.

The housing material is Kovar, a ferromagnetic Fe-Ni-Co alloy that features a modest heat conductivity of approx. 17 W/(K·m) a Young's modulus of approx. 150 GPa and a coefficient of linear expansion of approx. 5 ppm/K at room temperature and well above. For the latter it is very well established for integration with AlN (coefficient of linear expansion approx. 4.7 ppm/K at room temperature and well above) in the field of electronic hybrids. Further, also as heritage from electronic hybrid technology, a glass-soldering technology exists that allows for integration of electrical feedthroughs into the housing. The housing shown in Figure 2 features a form factor of 175×75×23 mm³ and a mass of approximately 750 g.

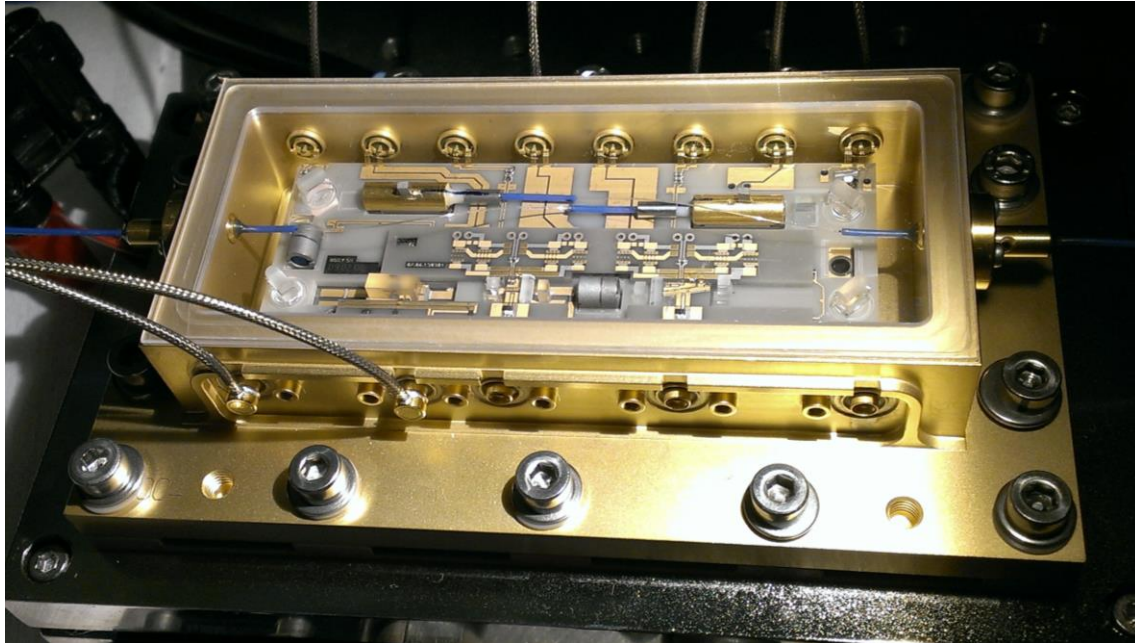


Figure 2. ECDL-MOPA laser module for operation at 780 nm. The photograph shows the AlN ceramic body, the housing as well as the optical and electrical feedthroughs.

We have developed isolated coaxial feedthroughs that provide an ampacity of 3 A direct current (DC) and an rf signal bandwidth well above 10 GHz in a 50Ω environment. Galvanic isolation from the housing helps to avoid electrostatic damage to the device, specifically to the laser diodes, and it eases measures against electro-magnetic interference (EMI). Each signal transduced from the inside to the outside of the module or *vice versa* is interfaced through its own isolated coaxial feedthrough. For high current applications, feedthroughs can be paralleled by proper Au-wire bonding on the ceramic module body.

In order to transmit the optical signals between inside and outside the module we selected an approach that relies on implementing fiber coupling already on the ceramic module body. An alternative, more common approach would have been to implement the fiber coupling unit (fiber and focusing lens) within the housing. However, this requires high mechanical stability between the ceramic module body and the housing. For example, relative beam pointing between the laser beam generated on the ceramic module and the optical axis of a fiber coupler integrated into the housing has been kept well below $100 \mu\text{rad}$ which we believe cannot be guaranteed with existing module designs in a realistic application environment. The requirements become even more stringent when smaller wavelengths are addressed.

We hence use a Kovar ferrule with a diameter of 4 mm that carries a pre-aligned focusing lens and a single mode, polarization maintain optical fiber. This rigid assembly is integrated into the ceramic module body. The optical fiber is fed through a flange attached to and sealed against the housing. The fiber itself is sealed against the flange by means of a low outgassing adhesive. The feedthrough maintains a polarization extinction ratio of more than 20 dB as long as the fiber is not under mechanical stress inside the module.

When all hybrid integration work has been completed the module housing is closed by seam welding with lid made of Kovar.

3. ECDL-MOPA LASER MODULE EMITTING AT 1064 NM

The JOKARUS experiment, successfully flown on the TEXUS54⁷ sounding rocket of the DLR on May 13th 2018, demonstrated the first iodine-based frequency reference in space. The laser source of the payload⁸ consisted of an ECDL-MOPA laser module operating at the central wavelength of 1064.49 nm. In the following, the electro-optical performance of the ECDL-MOPA laser module shall be presented⁹.

The electro-optical performance of the ECDL-MOPA has been investigated at a heat sink temperature of 25 °C. The VHBG temperature has been set to 25 °C to allow for emission around 1064 nm. The spectral parameters of the ECDL-MOPA are dominated by the characteristics of the ECDL master oscillator. The wavelength tuning with the injection current of the ECDL diode laser chip (RWL) for a constant injection current of the ridge-waveguide amplifier (RWA, 1500 mA) is depicted in Figure 3. It is shown, that for a RWL injection current of approx. 100 mA, the target wavelength of 1064.49 nm is met. A side-mode suppression of better than 45 dB has been achieved.

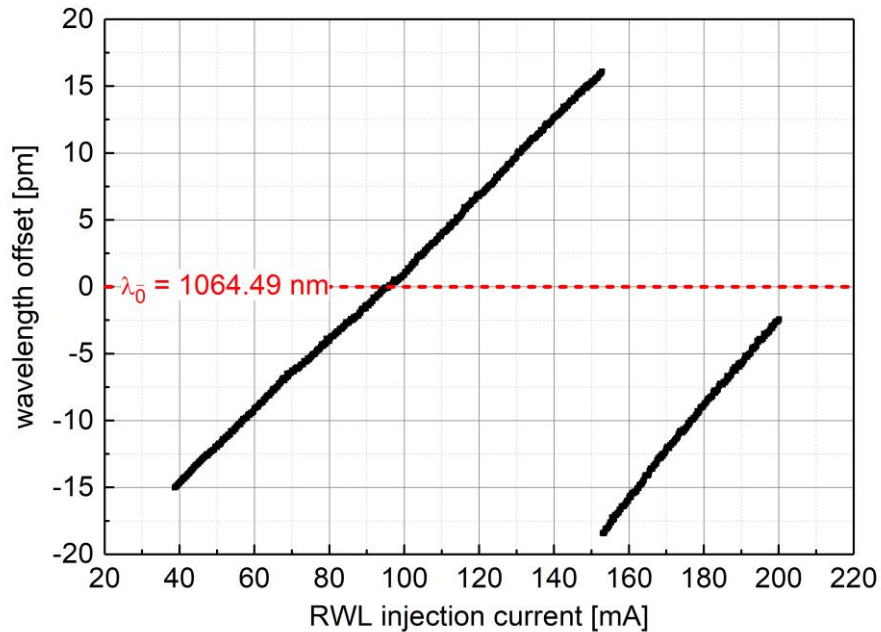


Figure 3. Wavelength tuning as function of injection current of ECDL diode laser chip (RWL) for a constant injection current of the PA (RWA) of ~ 1500 mA.

The spectral stability has been investigated using a self-delayed heterodyne setup with a delay line of 2 km length (~ 10 μs) by recording of the beat note in the time domain with an IQ measurement tool¹⁰. The resulting frequency noise power spectral density (PSD) is shown in Figure 4. Delay line artefacts can be seen at offset frequencies of 100 kHz and its harmonics. From the white noise floor, a Lorentzian linewidth of about 630 Hz can be estimated. The corresponding technical linewidth (FWHM level) measures about 30 kHz estimated from the frequency noise PSD according to the method proposed by Di Domenico et al.¹¹.

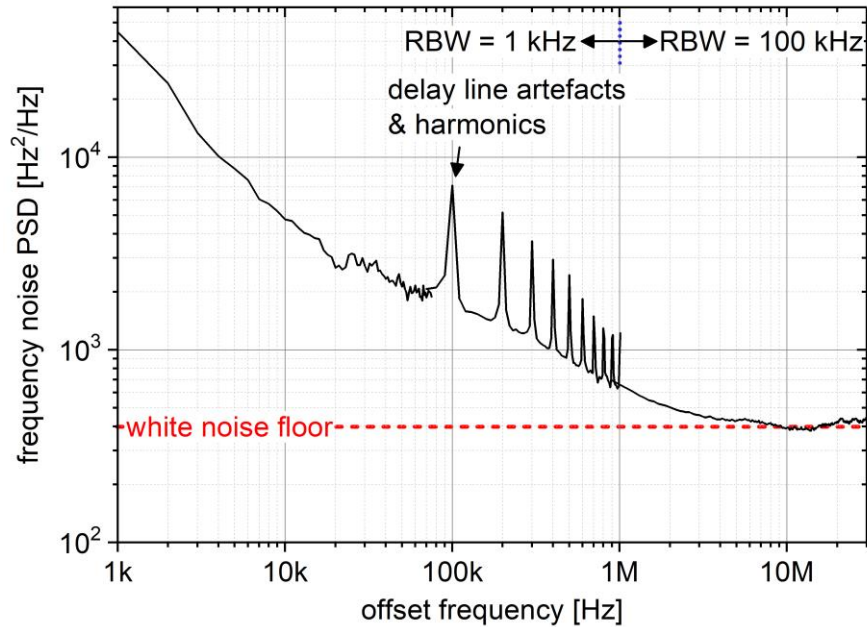


Figure 4. . Frequency noise PSD of ECDL-MOPA laser module for a RWL injection current of approx. 100 mA and RWA injection current of ~ 1500 mA.

The ex-fiber optical power of the ECDL-MOPA module (front output) is shown in Figure 5 for a constant injection current into the RWL chip and varying injection current into the RWA chip. It can be seen that a fiber-coupled optical power in excess of 500 mW can be reached. The rear output of the laser offers about 4 mW for e.g. monitoring purposes.

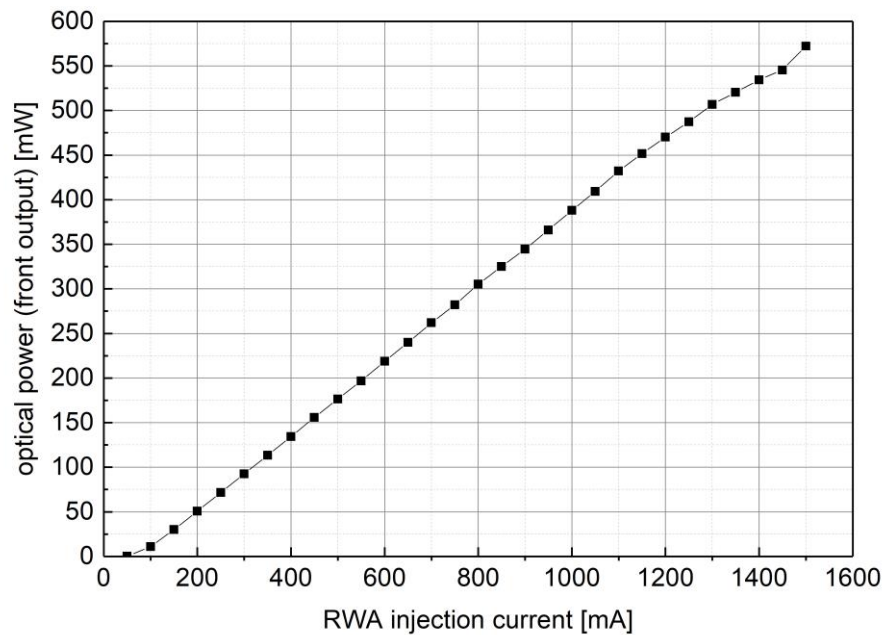


Figure 5. Optical power of ECDL-MOPA (ex-fiber) for a constant injection current into the RWL of ~ 100 mA.

4. SUMMARY AND OUTLOOK

In this paper, a versatile technology platform that can accommodate different laser architectures comprising 2 arbitrary diode laser chips has been presented. Based on an AlN substrate, the micro-optical bench can accommodate diode laser chips, micro-optics, on-board fiber couplers, discrete electronics and mini thermo-electric coolers, so as to form a hybrid micro-integrated laser module. The packaging of the micro-optical bench into a Kovar housing and the electrical and optical feedthroughs have also been described.

Based on the technology platform mentioned above, an ECDL-MOPA laser module has been realized, that emits more than 570 mW optical power ex-fiber at the emission wavelength of 1064.49 nm. The FWHM laser linewidth at this working point is shown to be below 30 kHz. This laser module has been successfully flown on a sounding rocket mission as part of an iodine-based frequency reference.

The next steps consist in the further development of the laser module technology for long-term missions on the ISS and on satellites. One central issue is the hermetic sealing of the laser module package, where concepts for the sealing of the housing and for hermetic fiber feedthroughs are being investigated. Moreover, the radiation hardness in a low-earth orbit mission scenario of central optical components such as the VHBG, micro-optical isolators or the fiber couplers are also being tested. In addition, the long-term reliability of the ECDL-MOPA laser concept needs to be investigated.

REFERENCES

- [1] T. van Zoest et al., "Bose-Einstein condensation in microgravity," *Science* 328, 1540–1543 (2010).
- [2] A. D. Ludlow, M. M. Boyd, J. Ye, E. Peik, and P. O. Schmidt, "Optical atomic clocks," *Rev. Mod. Phys.* 87, 637–701 (2015).
- [3] I. Dutta et al., "Continuous cold-atom inertial sensor with 1nrad/sec rotation stability," *Phys. Rev. Lett.* 116, 183003 (2016).
- [4] D. N. Aguilera et al., "STE-QUEST – test of the universality of free fall using cold atom interferometry," *Class. Quantum Gravity* 31, 115010 (2014).
- [5] P. Hamilton, M. Jaffe, P. Haslinger, Q. Simmons, H. Müller, and J. Khoury, "Atom-interferometry constraints on dark energy," *Science*, vol. 349, pp. 849–851, 2015.
- [6] M. Schiemangk et al., "High-power, micro-integrated diode laser modules at 767 and 780 nm for portable quantum gas experiments," *Appl. Opt.* 54, 5332–5338 (2015)
- [7] DLR, "Successful completion of the TEXUS 54/55 dual rocket mission", 05 June 2018, https://www.dlr.de/dlr/en/desktopdefault.aspx/tabid-10081/151_read-27969/year-all/#/gallery/30739
- [8] V. Schkolnik et al., "JOKARUS – design of a compact optical iodine frequency reference for a sounding rocket mission," *EPJ Quantum Technol.* 4(9), (2017).
- [9] Christopher, H. et al., "Narrow linewidth micro-integrated high power diode laser module for deployment in space", *IEEE ICSOS*, 978-1-5090-6511-0/17 (2017)
- [10] M. Schiemangk, S. Spießberger, A. Wicht, G. Erbert, G. Tränkle, and A. Peters, "Accurate frequency noise measurement of free-running lasers," *Appl. Opt.* 53, 7138–7143 (2014).
- [11] G. Di Domenico, S. Schilt, and P. Thomann, "Simple approach to the relation between laser frequency noise and laser line shape," *Appl. Opt.* 49, 4801–4807 (2010).